Oscillatory tunneling magnetoresistance in magnetic tunnel junctions with inserted nonmagnetic layer

Changsik Choi and Byung Chan Lee[*]

Department of Physics, Inha University, Incheon 402-751, Republic of Korea

(Received 19 June 2012; published 11 October 2012)

Oscillatory tunneling magnetoresistance (TMR) as a function of spacer thickness is investigated theoretically for a magnetic tunnel junction with a nonmagnetic layer inserted between the tunnel barrier and the ferromagnetic layer. TMR is characterized in an analytical form, that is expressed with the transmission and reflection amplitudes of single interfaces at the Fermi level, and by the extremal wave vectors. Electronic structures with multiple bands are taken into account in the derivation characterizing the TMR, and the proposed analytical expression can be directly applied to real junctions. Based on our model, the features of TMR dependence on spacer thickness are discussed, including selection rules for the oscillation period. Numerical calculations are performed using an envelope-function theory for several cases, and we show that our model is in good agreement with the exact result.

I. INTRODUCTION

Since high tunneling magnetoresistance (TMR) was first observed at room temperature,[1] magnetic tunnel junctions (MTJs) have been a focus of interest. Extensive research has been carried out to understand and improve the properties of MTJs. A huge increase in TMR with lower junction resistance was achieved when AlO_x tunnel barriers were replaced by MgO, and this was followed by realizations of memory devices based on MTJs with MgO barriers.[2] Tunneling current in the MTJ is spin polarized, which adds another dimension to the tunneling effect, and scientific attention has thus been drawn to the spin-dependent tunneling phenomenon. When a nonmagnetic (NM) layer is inserted between a ferromagnetic (FM) layer and the insulating (I) tunnel barrier of the MTJ, the spin polarization of the tunneling current changes and the TMR is directly affected. An early theoretical work predicted the oscillatory TMR as a function of the NM thickness due to the quantum well states inside the NM layer.[3] In sputtered samples, it has been shown that an NM layer between the tunnel barrier and FM layer could be detrimental to TMR, and the TMR decreases as a function of NM thickness.[4,5] These experimental results have been explained theoretically with a free electron model, and the decay of TMR was attributed to a loss of coherence in the electron propagation.[6] Different experimental results have been obtained for a crystalline NM layer inserted between the tunnel barrier and the FM layer. Yuasa *et al.*[7] experimentally investigated the dependence of TMR on Cu thickness in $NiFe/AlO_x/Cu/Co$ junctions with samples grown by molecular beam epitaxy. They found that the TMR decayed but oscillated as a function of Cu thickness. The oscillation period was determined by the nesting feature of the Cu Fermi surface. This oscillatory TMR has been investigated theoretically based on a single-band tight-binding model, a free-electron model, and full-band calculations.[8–19] Many features have been explained with calculations using simple models, but direct comparisons with the experimental data are difficult because realistic electronic structures were not considered. The full-band calculations are very useful for the description of real systems. However they are time consuming, and sometimes it is not easy to understand the underlying physics. Furthermore, full-band calculations are usually carried out for an ideal situation, and significant discrepancies often occur between theory and experiments.

We introduce an analytical expression that describes the dependence of TMR on NM thickness for FM/I/NM/FM junctions based on full-band structures. Our approach uses the generalization of a previously described single-band case[19] to a multiple-band case that considers the real materials. The TMR is expressed with transmission and reflection amplitudes of single interfaces at the Fermi level, and extremal wave vectors. The full-band structures of the materials are taken into account in our proposed model, and the calculation of several transmission and reflection amplitudes with real band structures can make a direct comparison with experimental results possible. Based on our model, selection rules for the oscillation period are discussed, and we suggest that very few oscillation periods will be observed in experiments even when there are many extremal spanning vectors of the NM Fermi surface. This situation is very different than the interlayer exchange coupling in magnetic multilayers. Our model explicitly shows that TMR dependence on NM thickness is affected by the thickness of the tunnel barrier, and predicts that the TMR will go to zero as the NM thickness increases. To check the validity of our model, we carried out numerical calculations using an envelope-function theory for several cases including NM material with a Fermi surface similar to the Cu(001) case. Although our model is calculated using the parameters at the Fermi level and the extremal wave vector, it is in good agreement with the exact numerical results.

II. THEORETICAL MODEL

Figure 1(a) shows a schematic diagram of an MTJ with an NM layer inserted between the tunnel barrier and the right magnetic layer [FM(R)]. The growth direction is taken as the z axis, and d is the thickness of the NM layer. We used a frozen potential approximation, and the eigenstate of the MTJ is expressed with linear combinations of the bulk states for each layer. We assumed that the wave-vector component parallel to the interface ($\mathbf{k}_\parallel$) is conserved throughout the MTJ.

A two-channel model was adopted and spin-flip scattering was ignored. The normalized bulk solution of the material for the left magnetic layer [FM(L)] is denoted as $|\varepsilon, \mathbf{k}_\parallel, k_{z,n\sigma}^{L+(-)}\rangle$ for a given energy ε and $\mathbf{k}_\parallel$, where k_z is the z component of the wave vector, n is the band index, σ is the spin index, and the $+$ $(-)$ sign is for the state traveling to the right (left). Similarly, the

bulk solutions of the FM(R) and NM materials are expressed as $|\varepsilon, \mathbf{k}_\parallel, k_{z,n\sigma}^{R+(-)}\rangle$ and $|\varepsilon, \mathbf{k}_\parallel, k_{z,n}^{N+(-)}\rangle$, respectively. Multiple bands are taken into account, and $2N_{L(R)\sigma}$ is the number of bulk states in the left (right) FM layer for a given ε, $\mathbf{k}_\parallel$, and spin σ. The number of bulk states in the NM layer for a given ε and $\mathbf{k}_\parallel$ is denoted as $2N_N$. The eigenstate of the MTJ is written as

$$
\big|\psi_\sigma(\varepsilon, \mathbf{k}_\parallel)\big\rangle =
\begin{cases}
\sum_{n=1}^{N_{L\sigma}} A_{n\sigma}^+ \dfrac{|\varepsilon, \mathbf{k}_\parallel, k_{z,n\sigma}^{L+}\rangle}{\sqrt{|v_{z,n\sigma}^{L+}|}} + \sum_{n=1}^{N_{L\sigma}} A_{n\sigma}^- \dfrac{|\varepsilon, \mathbf{k}_\parallel, k_{z,n\sigma}^{L-}\rangle}{\sqrt{|v_{z,n\sigma}^{L-}|}}, & z < 0, \\[3mm]
\sum_{n=1}^{N_N} C_{n\sigma}^+ \dfrac{|\varepsilon, \mathbf{k}_\parallel, k_{z,n}^{N+}\rangle}{\sqrt{|v_{z,n}^{N+}|}} + \sum_{n=1}^{N_N} C_{n\sigma}^- \dfrac{|\varepsilon, \mathbf{k}_\parallel, k_{z,n}^{N-}\rangle}{\sqrt{|v_{z,n}^{N-}|}}, & b < z < b + d, \\[3mm]
\sum_{n=1}^{N_{R\sigma}} B_{n\sigma}^+ \dfrac{|\varepsilon, \mathbf{k}_\parallel, k_{z,n\sigma}^{R+}\rangle}{\sqrt{|v_{z,n\sigma}^{R+}|}} + \sum_{n=1}^{N_{R\sigma}} B_{n\sigma}^- \dfrac{|\varepsilon, \mathbf{k}_\parallel, k_{z,n\sigma}^{R-}\rangle}{\sqrt{|v_{z,n\sigma}^{R-}|}}, & z > b + d,
\end{cases}
\tag{1}
$$

where v_z is the z component of the group velocity [$v_z = (1/\hbar)(\partial \varepsilon / \partial k_z)$] for the corresponding bulk eigenstate, and $A_{n\sigma}^\pm$, $C_{n\sigma}^\pm$, and $B_{n\sigma}^\pm$ are coefficients to be determined from the boundary conditions. Note that the bases in Eq. (1) are adjusted so that the current is normalized. The eigenstate inside the tunnel barrier is not shown here. We define vectors $\mathbf{A}_\sigma^\pm$ and $\mathbf{B}_\sigma^\pm$ as $\mathbf{A}_\sigma^\pm \equiv (A_{1\sigma}^\pm, A_{2\sigma}^\pm, \dots, A_{N_{L\sigma}\sigma}^\pm)^T$ and $\mathbf{B}_\sigma^\pm \equiv (B_{1\sigma}^\pm, B_{2\sigma}^\pm, \dots, B_{N_{R\sigma}\sigma}^\pm)^T$. Then, $\mathbf{A}_\sigma^-$ and $\mathbf{B}_\sigma^+$ are related to $\mathbf{A}_\sigma^+$ and $\mathbf{B}_\sigma^-$ by the S matrix,[20]

$$
\begin{pmatrix} \mathbf{A}_\sigma^- \\ \mathbf{B}_\sigma^+ \end{pmatrix} = \begin{pmatrix} \mathbf{r}_\sigma & \mathbf{t}_\sigma' \\ \mathbf{t}_\sigma & \mathbf{r}_\sigma' \end{pmatrix} \begin{pmatrix} \mathbf{A}_\sigma^+ \\ \mathbf{B}_\sigma^- \end{pmatrix}.
\tag{2}
$$

Matrix element $t_{\sigma,nn'}$ $(r_{\sigma,nn'})$ is a kind of transmission (reflection) amplitude for an incoming wave from the left $|\varepsilon, \mathbf{k}_\parallel, k_{z,n'\sigma}^{L+}\rangle$ to be transmitted (reflected) to $|\varepsilon, \mathbf{k}_\parallel, k_{z,n\sigma}^{R+}\rangle$ $(|\varepsilon, \mathbf{k}_\parallel, k_{z,n\sigma}^{L-}\rangle)$. The transmission (reflection) amplitude for the opposite direction is given by $t_{\sigma,nn'}'$ $(r_{\sigma,nn'}')$. We calculated the conductance G for low bias and zero temperature from the Landauer-Büttiker formalism as follows:

$$
G = \frac{e^2}{h} \sum_{\mathbf{k}_\parallel, \sigma} \text{Tr}[\mathbf{t}_\sigma^\dagger(\varepsilon_F, \mathbf{k}_\parallel) \mathbf{t}_\sigma(\varepsilon_F, \mathbf{k}_\parallel)],
\tag{3}
$$

where ε_F is the Fermi energy. As shown in Figs. 1(b) and 1(c), we considered the FM(L)/I/NM and NM/FM(R) interfaces separately, and expressed $\mathbf{t}_\sigma$ of the MTJ with the transmission and reflection amplitudes of each separated interface. The eigenstate of the FM(L)/I/NM system shown in Fig. 1(b) is expressed as

$$
\big|\psi_\sigma^L(\varepsilon, \mathbf{k}_\parallel)\big\rangle =
\begin{cases}
\sum_{n=1}^{N_{L\sigma}} A_{n\sigma}^{L+} \dfrac{|\varepsilon, \mathbf{k}_\parallel, k_{z,n\sigma}^{L+}\rangle}{\sqrt{|v_{z,n\sigma}^{L+}|}} + \sum_{n=1}^{N_{L\sigma}} A_{n\sigma}^{L-} \dfrac{|\varepsilon, \mathbf{k}_\parallel, k_{z,n\sigma}^{L-}\rangle}{\sqrt{|v_{z,n\sigma}^{L-}|}}, & z < 0, \\[3mm]
\sum_{n=1}^{N_N} C_{n\sigma}^{L+} \dfrac{|\varepsilon, \mathbf{k}_\parallel, k_{z,n}^{N+}\rangle}{\sqrt{|v_{z,n}^{N+}|}} + \sum_{n=1}^{N_N} C_{n\sigma}^{L-} \dfrac{|\varepsilon, \mathbf{k}_\parallel, k_{z,n}^{N-}\rangle}{\sqrt{|v_{z,n}^{N-}|}}, & z > b,
\end{cases}
\tag{4}
$$

where $A_{n\sigma}^{L\pm}$ and $C_{n\sigma}^{L\pm}$ are coefficients. We define $\mathbf{A}_\sigma^{L\pm} \equiv (A_{1\sigma}^{L\pm}, A_{2\sigma}^{L\pm}, \dots, A_{N_{L\sigma}\sigma}^{L\pm})^T$ and $\mathbf{C}_\sigma^{L\pm} \equiv (C_{1\sigma}^{L\pm}, C_{2\sigma}^{L\pm}, \dots, C_{N_N\sigma}^{L\pm})^T$, and the relation between the coefficients is expressed as

$$
\begin{pmatrix} \mathbf{A}_\sigma^{L-} \\ \mathbf{C}_\sigma^{L+} \end{pmatrix} = \begin{pmatrix} \mathbf{r}_\sigma^L & \mathbf{t}_\sigma'^L \\ \mathbf{t}_\sigma^L & \mathbf{r}_\sigma'^L \end{pmatrix} \begin{pmatrix} \mathbf{A}_\sigma^{L+} \\ \mathbf{C}_\sigma^{L-} \end{pmatrix}.
\tag{5}
$$

Similarly, for the NM/FM interface shown in Fig. 1(c), the eigenstate is given by

$$
\big|\psi_\sigma^R(\varepsilon, \mathbf{k}_\parallel)\big\rangle =
\begin{cases}
\sum_{n=1}^{N_N} C_{n\sigma}^{R+} \dfrac{|\varepsilon, \mathbf{k}_\parallel, k_{z,n}^{N+}\rangle}{\sqrt{|v_{z,n}^{N+}|}} + \sum_{n=1}^{N_N} C_{n\sigma}^{R-} \dfrac{|\varepsilon, \mathbf{k}_\parallel, k_{z,n}^{N-}\rangle}{\sqrt{|v_{z,n}^{N-}|}}, & z < 0, \\[3mm]
\sum_{n=1}^{N_{R\sigma}} B_{n\sigma}^{R+} \dfrac{|\varepsilon, \mathbf{k}_\parallel, k_{z,n\sigma}^{R+}\rangle}{\sqrt{|v_{z,n\sigma}^{R+}|}} + \sum_{n=1}^{N_{R\sigma}} B_{n\sigma}^{R-} \dfrac{|\varepsilon, \mathbf{k}_\parallel, k_{z,n\sigma}^{R-}\rangle}{\sqrt{|v_{z,n\sigma}^{R-}|}}, & z > 0.
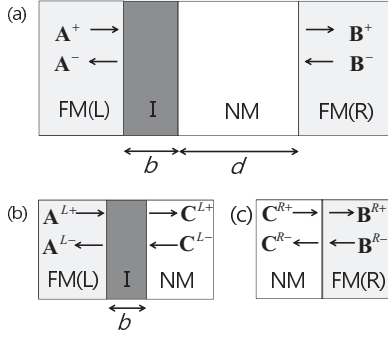\end{cases}
\tag{6}
$$

FIG. 1. (a) Schematic diagram of a magnetic tunnel junction (MTJ) with a nonmagnetic (NM) layer inserted between the insulating (I) tunnel barrier and the right ferromagnetic layer [FM(R)]. d is the thickness of the NM layer. $\mathbf{A}^+$, $\mathbf{A}^-$, $\mathbf{B}^+$, and $\mathbf{B}^-$ are coefficient vectors [see Eq. (1)]. The transmission in the MTJ can be expressed with the reflection and transmission amplitudes of the separated interfaces shown in (b) and (c).

The vectors $\mathbf{C}_\sigma^{R\pm} = (C_{1\sigma}^{R\pm}, C_{2\sigma}^{R\pm}, \ldots, C_{N_N\sigma}^{R\pm})^T$ and $\mathbf{B}_\sigma^{R\pm} = (B_{1\sigma}^{R\pm}, B_{2\sigma}^{R\pm}, \ldots, B_{N_{R_\sigma}\sigma}^{R\pm})^T$ are related as follows:

$$\begin{pmatrix} \mathbf{C}_\sigma^{R-} \\ \mathbf{B}_\sigma^{R+} \end{pmatrix} = \begin{pmatrix} \mathbf{r}_\sigma^R & \mathbf{t}'^R_\sigma \\ \mathbf{t}_\sigma^R & \mathbf{r}'^R_\sigma \end{pmatrix} \begin{pmatrix} \mathbf{C}_\sigma^{R+} \\ \mathbf{B}_\sigma^{R-} \end{pmatrix}. \quad (7)$$

$\mathbf{r}$ and $\mathbf{t}$ of the MTJ in Eq. (2) can be expressed with $\mathbf{r}^L$, $\mathbf{t}^L$, $\mathbf{r}'^L$, and $\mathbf{t}'^L$ in Eq. (5) and $\mathbf{r}^R$, $\mathbf{t}^R$, $\mathbf{r}'^R$, and $\mathbf{t}'^R$ in Eq. (7) by considering the multiple reflection inside the NM. We introduce the mean free path λ due to scattering inside the NM layer. For simplicity, we assumed that λ is constant, although the dependence of λ on other parameters can be included in our calculation. Then, the phase-coherent part of the reflection amplitude $\mathbf{r}^c$ is given by

$$\mathbf{r}^c = \mathbf{r}_\sigma^L + \mathbf{t}'^L_\sigma \rho_\sigma^R \tau_\sigma^L e^{-2d/\lambda} + \sum_{n=1}^{\infty} \mathbf{t}'^L_\sigma \left(\rho_\sigma^R \rho'^L_\sigma \right)^n \rho_\sigma^R \tau_\sigma^L e^{-(2d/\lambda)(n+1)}, \quad (8)$$

where the matrix elements $\rho_{\sigma,nn'}^R$, $\tau_{\sigma,nn'}^L$, and $\rho'^L_{\sigma,nn'}$ are $\rho_{\sigma,nn'}^R = e^{-ik_{z,n}^{N-}d} r_{\sigma,nn'}^R$, $\tau_{\sigma,nn'}^L = e^{ik_{z,n}^{N+}d} t_{\sigma,nn'}^L$, and $\rho'^L_{\sigma,nn'} = e^{ik_{z,n}^{N+}d} r'^L_{\sigma,nn'}$. The phase-coherent part of the transmission amplitude $\mathbf{t}^c$ can be obtained in a similar way. Because of the scattering inside the NM layer, we have $\text{Tr}[\mathbf{t}^{c\dagger}\mathbf{t}^c] + \text{Tr}[\mathbf{r}^{c\dagger}\mathbf{r}^c] < 1$ and we need to include the diffusive part of the transport. We assume that the transmission back to the FM(L) layer through the tunnel barrier is much smaller than that through the NM/FM(R) interface. Then, the $1 - \text{Tr}[\mathbf{t}^{c\dagger}\mathbf{t}^c] - \text{Tr}[\mathbf{r}^{c\dagger}\mathbf{r}^c]$ portion contributes to the sequential transmission.[12] Adding the coherent and sequential transmissions, we have $\text{Tr}[\mathbf{t}^\dagger\mathbf{t}] = 1 - \text{Tr}[\mathbf{r}^{c\dagger}\mathbf{r}^c]$. Finally, using the properties of the S matrix and taking the first-order term in $e^{-2d/\lambda}$, we obtain

$$\text{Tr}[\mathbf{t}^\dagger\mathbf{t}] \cong \text{Tr}[\mathbf{t}^{L\dagger}\mathbf{t}^L] + 2\text{Re}\,\text{Tr}[\mathbf{t}_\sigma^{L\dagger} \mathbf{r}'^L_\sigma \rho_\sigma^R \tau_\sigma^L] e^{-2d/\lambda}. \quad (9)$$

Even when λ is very large, this is a reasonable approximation because the magnitude of the matrix element $r_{\sigma,nn'}^R$ is less than 1, and the higher-order terms are more rapidly oscillating as functions of d and consequently contribute less to the

conduction. The conductance is given by

$$G = G_0 + \frac{2e^2}{h} e^{-2d/\lambda} \text{Re} \sum_{\mathbf{k}_\parallel,\sigma} \text{Tr}[\mathbf{t}_\sigma^{L\dagger} \mathbf{r}'^L_\sigma \rho_\sigma^R \tau_\sigma^L], \quad (10)$$

where G_0 is the conductance of the FM(L)/I/NM junctions and the energy is set to the Fermi level ($\varepsilon = \varepsilon_F$). The conductance depends on the magnetic configurations, and we denote the conductance for parallel (antiparallel) magnetization of two magnetic layers as $G_{P(AP)}$. The TMR is given by $\Delta G/G_{AP}$, where ΔG is $\Delta G = G_P - G_{AP}$. Here, we will show the calculation of ΔG, and $G_{P(AP)} - G_0$ can be obtained in the same way. We define $\Delta T_{nn'}^L$ and $\Delta r_{nn'}^R$ as $\Delta T_{nn'}^L = (\mathbf{t}_\uparrow^L \mathbf{t}_\uparrow^{L\dagger} \mathbf{r}'^L_\uparrow - \mathbf{t}_\downarrow^L \mathbf{t}_\downarrow^{L\dagger} \mathbf{r}'^L_\downarrow)_{nn'} = |\Delta T_{nn'}^L| e^{i\phi_{nn'}^L}$ and $\Delta r_{nn'}^R = (r_{\uparrow,nn'}^R - r_{\downarrow,nn'}^R)/2 = |\Delta r_{nn'}^R| e^{i\phi_{nn'}^R}$, where $\uparrow$ ($\downarrow$) is the majority (minority) spin. ΔG is expressed as

$$\Delta G = \frac{4e^2}{h} e^{-2d/\lambda} \text{Re} \sum_{n,n'} \sum_{\mathbf{k}_\parallel,\sigma} |\Delta T_{nn'}^L| |\Delta r_{nn'}^R| e^{i(q_{nn'}d + \phi_{nn'})}, \quad (11)$$

where $q_{nn'}$ and $\phi_{nn'}$ are $q_{nn'} = k_n^{N+} - k_{n'}^{N-}$ and $\phi_{nn'} = \phi_{nn'}^L + \phi_{nn'}^R$.

The summation over $\mathbf{k}_\parallel$ can be performed in a manner similar to the calculation of the interlayer exchange coupling in magnetic multilayers.[21,22] $|\Delta T_{nn'}^L|$ and $e^{iq_{nn'}^F d}$ are rapidly changing as functions of $\mathbf{k}_\parallel$. We assume the exponential dependence of $|\Delta T_{nn'}^L|$ such that $|\Delta T_{nn'}^L| \propto e^{-b\chi_{nn'}(\mathbf{k}_\parallel)}$. Suppose that $(k_{\alpha x}, k_{\alpha y})$ is an extremal point, which means $\nabla_{\mathbf{k}_\parallel}[-b\chi_{nn'} + i(q_{nn'}d + \phi_{nn'})] = 0$ at $\mathbf{k}_\parallel = (k_{\alpha x}, k_{\alpha y})$. Since the main contribution to the integral comes from the vicinity of the extremal point, we expand $-b\chi_{nn'} + i(q_{nn'}d + \phi_{nn'})$ around the extremal point as follows:

$$-b\chi_{nn'} + i(q_{nn'}d + \phi_{nn'})$$
$$\approx -b\chi_\alpha + i(q_\alpha d + \phi_\alpha) - \left(\frac{b}{\kappa_{\alpha x}^b} - i \frac{d + d_{\alpha x}}{\kappa_{\alpha x}^d} \right)(k_x - k_{\alpha x})^2$$
$$- \left(\frac{b}{\kappa_{\alpha y}^b} - i \frac{d + d_{\alpha y}}{\kappa_{\alpha y}^d} \right)(k_y - k_{\alpha y})^2, \quad (12)$$

where new parameters $\frac{1}{\kappa_{\alpha x}^b} = \frac{1}{2} \frac{\partial^2 \chi_{nn'}}{\partial k_x^2}$, $\frac{1}{\kappa_{\alpha y}^b} = \frac{1}{2} \frac{\partial^2 \chi_{nn'}}{\partial k_y^2}$, $\frac{1}{\kappa_{\alpha x}^d} = \frac{1}{2} \frac{\partial^2 q_{nn'}}{\partial k_x^2}$, $\frac{1}{\kappa_{\alpha y}^d} = \frac{1}{2} \frac{\partial^2 q_{nn'}}{\partial k_y^2}$, $d_{\alpha x} = \frac{1}{2} \kappa_{\alpha x}^d \frac{\partial^2 \phi_{nn'}}{\partial k_x^2}$, and $d_{\alpha y} = \frac{1}{2} \kappa_{\alpha y}^d \frac{\partial^2 \phi_{nn'}}{\partial k_y^2}$ are evaluated at $\varepsilon = \varepsilon_F$ and $\mathbf{k}_\parallel = (k_{\alpha x}, k_{\alpha y})$. Then, the summation over $\mathbf{k}_\parallel$ is carried out analytically and ΔG is given by

$$\Delta G = \frac{e^2}{h\pi} e^{-2d/\lambda} \text{Re} \sum_\alpha \frac{n_\alpha |\Delta T_\alpha^L| |\Delta r_\alpha^R| e^{i(q_\alpha d + \phi_\alpha)}}{\sqrt{\frac{b}{\kappa_{\alpha x}^b} - i \frac{d + d_{\alpha x}}{\kappa_{\alpha x}^d}} \sqrt{\frac{b}{\kappa_{\alpha y}^b} - i \frac{d + d_{\alpha y}}{\kappa_{\alpha y}^d}}}, \quad (13)$$

where n_α is the number of the extremal points of the same kind. The phase of the square root is taken from $-\pi/2$ to $\pi/2$. The parameters in Eq. (13) are evaluated at the Fermi level and the extremal point. Suppose we have $\nabla_{\mathbf{k}_\parallel} \chi = 0$ at $\mathbf{k}_\parallel^b = (k_x^b, k_y^b)$ and $\nabla_{\mathbf{k}_\parallel}(qd + \phi) = 0$ at $\mathbf{k}_\parallel^d = (k_x^d, k_y^d)$. In general, $\mathbf{k}_\parallel^b$ is different from $\mathbf{k}_\parallel^d$ and the corresponding extremal point $(k_{\alpha x}, k_{\alpha y})$ is a complex number. This makes other parameters such as q_α complex numbers, and the situation is rather

complicated. However, when $\mathbf{k}_\parallel^b$ and $\mathbf{k}_\parallel^d$ are far apart, the contribution is negligible because of small $|\Delta T_\alpha^L|$. The most important case is when $\mathbf{k}_\uparrow^b$ and $\mathbf{k}_\uparrow^d$ coincide. This is expected to happen often at $\mathbf{k}_\parallel = 0$ due to symmetry. In this case, $k_{\alpha x}$ and $k_{\alpha y}$ are real and ΔG becomes

$$\Delta G = \frac{e^2 n_\alpha}{2h\pi} \mathrm{Re} \frac{(|t_\uparrow^L|^2 - |t_\downarrow^L|^2)|r_\uparrow^R - r_\downarrow^R|e^{-2d/\lambda}e^{i(q_\alpha d + \phi_\alpha)}}{\sqrt{\frac{b}{\kappa_{\alpha x}^b} - i\frac{d+d_{\alpha x}}{\kappa_{\alpha x}^d}}\sqrt{\frac{b}{\kappa_{\alpha y}^b} - i\frac{d+d_{\alpha y}}{\kappa_{\alpha y}^d}}},$$
(14)

where we used $r_\uparrow'^L \cong r_\downarrow'^L$ with $|r_\uparrow'^L| \cong 1$, which is expected for a typical thickness of the tunnel barrier. In this case, q_α is exactly the extremal spanning vector of the NM Fermi surface.

The extremal spanning vector q_α of the NM Fermi surface gives rise to the period of the TMR oscillation. In principle, multiple periods are possible depending on the shape of the NM Fermi surface. However, the extremal spanning vectors of the NM Fermi surface are the necessary condition for TMR oscillation, and the period would be observed only when the corresponding $|\Delta T_\alpha^L|$ is large enough. Except for the symmetry point in $\mathbf{k}_\parallel$ space, the extremal points of the NM Fermi surface hardly coincide with the maxima point of $|\Delta T_\alpha^L|$ of the tunnel barrier. Thus, only few periods would be observable among the possible periods from the extremal spanning vectors. Compared with the oscillation of the interlayer exchange coupling for a corresponding spacer, fewer periods would be observed in TMR oscillation. Moreover, as b increases, $|\Delta T_\alpha^L|$ decreases rapidly as a function of $\mathbf{k}_\parallel$ away from the maxima. Thus, the multiple periods would be more difficult to observe for a thicker tunnel barrier. Since $|\Delta T_\alpha^L|$ is material dependent, the period of TMR oscillation could change for a different tunneling barrier. In Eq. (14), the extra phase factor arises from the square root in the denominator. This extra phase factor is d dependent, and the measured oscillation period will be slightly different from $2\pi/q_\alpha$. For instance, the period of TMR oscillation for NiFe/AlO$_x$/Cu(001)/Co is expected to be slightly smaller than $2\pi/q_\alpha$, which is the period of the interlayer exchange coupling for fcc Co/Cu(001)/Co multilayers.

We considered the observable periods with the assumption that the tunneling probability is maximum at $\mathbf{k}_\parallel = 0$. Then, only the oscillation for the extremal spanning vector at $\mathbf{k}_\parallel = 0$ would be observed. In NiFe/AlO$_x$/Cu(001)/Co junctions, there are two possible periods from the Fermi surface of Cu along the (001) direction. The long period is from the extremal spanning vector at $\mathbf{k}_\parallel = 0$, and the extremal vector for the short period is far away from $\mathbf{k}_\parallel = 0$. Thus, the short period is intrinsically invisible, and only the long period could be observed. There are four possible oscillation periods in NiFe/AlO$_x$/Cu(110)/Co junctions from the Cu Fermi surface along the (110) direction.[21] Among them, the only observable period is the extremal spanning vector corresponding to $\mathbf{k}_\parallel = 0$. This period is very short and would be easily wiped out by the interface roughness. Thus, it would be difficult to observe a TMR oscillation in this system. There is only one possible period for Cu(111),[21,22] and this period has been observed experimentally in the interlayer exchange coupling of Co/Cu(111)/Co multilayers.[23] However, this period would not be observed in NiFe/AlO$_x$/Cu(111)/Co

junctions because the corresponding extremal spanning vector is far from $\mathbf{k}_\parallel = 0$. Therefore, except for the long period of NiFe/AlO$_x$/Cu(001)/Co junctions, it would be difficult to observe a TMR oscillation as a function of Cu thickness. The situation for the Au and Ag spacers will be same as in the case of Cu because the shapes of the Fermi surfaces are similar. In the Fe/Cr/Fe multilayers, the long periods of interlayer coupling oscillation have been observed as a function of the Cr thickness for the (100), (110), and (211) orientations.[23] However, these long periods would not be observed experimentally in Fe/AlO$_x$/Cr/Fe or Fe/MgO/Cr/Fe tunnel junctions because the long periods are from the N point of the Cr Fermi surface,[24,25] which is away from $\mathbf{k}_\parallel = 0$ for any orientation. In experiments, this long period has not been observed for Fe/AlO$_x$/Cr(001)/Fe (Ref. 26) and Fe/MgO/Cr(001)/Fe (Ref. 27) tunnel junctions. Usually, the long period is clearly observed because it is not eliminated by the interface roughness. Although we discussed the case that the tunneling is dominated by perpendicularly incident electrons, the analysis is similar when the tunneling probability is maximum or high away from $\mathbf{k}_\parallel = 0$. If the dependence of the tunneling probability on $\mathbf{k}_\parallel$ changes with a different tunnel barrier, the TMR dependence on the NM spacer will be altered accordingly. Still, the crucial criterion is whether the tunneling probability is significant or not at the point of the extremal spanning vectors of the NM Fermi surface in the $\mathbf{k}_\parallel$ space. Except special points, the chances are that the point of the maximum tunneling probability does not coincide with the position of the extremal spanning vectors of the NM Fermi surface in the $\mathbf{k}_\parallel$ space. Thus many oscillations inferred from the NM Fermi surface would not be observed. When the tunnel barrier is extremely thin, the situation can be much different because the tunneling probability dependence on $\mathbf{k}_\parallel$ may change significantly. More oscillation periods can be observed with thinner tunnel barriers. Even in this case, the oscillation periods associated with relatively high tunneling probability will be observed.

Without the scattering effect, ΔG and TMR decays as $1/d$ for a thick NM layer. However, for thin NM layers, the decay rate is slower than $1/d$ and is affected by the tunnel barrier thickness b, and also by $d_{\alpha x}$ and $d_{\alpha y}$ ($\mathbf{k}_\parallel$ dependence of the reflection-amplitude phase factors). The amplitude decays much more slowly than $1/d$ for coherent transport when d is of the same order of magnitude as b. In experiments, the TMR oscillation decays much faster than $1/d$, which seems to be due to scattering. As the NM thickness increases, our model predicts that ΔG and TMR go to zero even when the mean free path (λ) is very long. We will address this point in Sec. III C.

III. NUMERICAL CALCULATION WITH AN ENVELOPE-FUNCTION THEORY

To test the validity of our model, we carried out numerical calculations based on an envelope-function theory for several cases. We used the same material for FM(L) and FM(R), and ignored scattering. The continuity of the wave function and the conservation of current at the interface were taken as the boundary conditions.
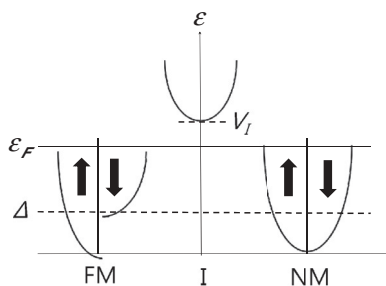
FIG. 2. Dispersion relation for the FM, I, and NM materials. Δ is the spin splitting inside the FM layer, V_I is the bottom energy for the tunnel barrier, and ε_F is the Fermi energy.

A. Effective-mass approximation

First, we considered the case that the dispersion relation of the NM material is the same as that of the FM material for majority spin. The dispersion relations of the FM material and the insulator are given by $\varepsilon(\mathbf{k}) = \hbar^2 k^2 / 2m_\sigma^* + V_\sigma$ and $\varepsilon(\mathbf{k}) = \hbar^2 k^2 / 2m_0 + V_I$, respectively, where m_σ^* is the spin-dependent effective mass of the FM material, m_0 is the bare electron mass, and V_I is the height of the tunnel barrier. We set $V_\uparrow = 0$ [$V_\downarrow = \Delta$] for the majority (minority) spin in the FM layer using the spin-splitting energy Δ. The effective mass of the FM material is $m_\uparrow = m_0$ for the majority spin and $m_\downarrow^* = m_0 \varepsilon_F / (\varepsilon_F - \Delta)$ for the minority spin. Schematics for
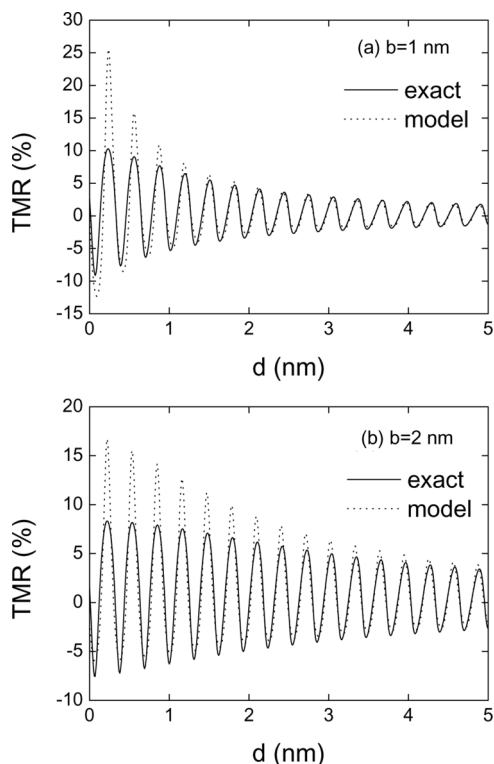

FIG. 3. TMR as a function of d for the effective-mass band. The barrier thicknesses are (a) $b = 1$ and (b) $b = 2$ nm. The parameters used in the calculation are $\varepsilon_F = 4$ eV, $V_I = 6$ eV, and $\Delta = 2.5$ eV. The effective mass of electrons with minority spin in the FM material is $m_\downarrow^* = m_0 \varepsilon_F / (\varepsilon_F - \Delta)$ and other effective masses are the bare electron mass m_0. The solid line is the exact result, and the dotted line is based on the proposed analytical formula.

the dispersion relations of the FM, I, and NM materials are shown in Fig. 2. Under these conditions, all the traveling states in the NM layer have corresponding traveling states in the FM layer, and total reflection does not occur at the NM/FM interface for any $\mathbf{k}_\parallel$. The parameters used in the calculation are $\varepsilon_F = 4$ eV, $V_I = 6$ eV, and $\Delta = 2.5$ eV. The TMR is plotted as a function of NM thickness d for the tunnel-barrier thicknesses of $b = 1$ nm and $b = 2$ nm in Figs. 3(a) and 3(b), respectively. The solid line represents the exact calculation, which was obtained using Eq. (3). The dotted line is the result of our analytical simple model described by Eq. (14). Note that the extremal point for the NM Fermi surface coincides with the maximum transmission point of the tunnel barrier at $\mathbf{k}_\parallel = 0$. When the NM layer is thin, there is some discrepancy between the exact result and our analytical model, but the agreement improves as the NM thickness increases. The overall trend of the NM thickness dependence is well depicted by our analytical model. The TMR oscillates and goes to zero as the NM thickness increases. It is also shown that the TMR dependence on d is affected by the thickness of the tunnel barrier. The peak points of TMR do not coincide for different tunnel barrier thicknesses. The decay of TMR as a function of d is faster for a thinner tunneling barrier. It is essential to consider the $\mathbf{k}_\parallel$ dependence of the transmission coefficient in the calculation. The effect of the tunnel barrier thickness on the NM thickness dependence of TMR is well described by our proposed analytical formula Eq. (14).

B. Spacer with nonparabolic dispersion relation

Second, to investigate the case of the multiple extremal spanning vectors in the NM layer, we assumed the following effective dispersion relation for the NM layer:

$$\varepsilon = \frac{1}{1-a^2} \left[\left(\frac{\hbar^2 k_\parallel^2}{2m_0} - a^2 \varepsilon_F \right)^2 + \left(\frac{\hbar^2 k_z^2}{2m_0} \right)^2 \right]^{1/2}, \quad (15)$$

where the constant a is set to $a = 0.68$. Except for the NM layer and $b = 1.5$ nm, the dispersion relations and parameters for the FM and tunnel barrier are the same as in the previous case. The effective mass and k_z in the NM layer were determined using Eq. (15). In Fig. 4(a), the cross section of the Fermi surface for bulk NM is plotted as a function of $k_\parallel$. There are two kinds of extremal spanning vectors: one at $k_\parallel = 0$ and the other at $k_\parallel = 0.68 k_F$, where $k_F = \sqrt{2m_0 \varepsilon_F} / \hbar$ is the magnitude of the Fermi wave vector for the FM with majority spin. The extremal spanning vector at $k_\parallel = 0$ ($k_\parallel = 0.68 k_F$) is shorter (longer) and can give rise to a long (short) period of the TMR oscillation, which is similar to the Cu(001) case. The TMR as a function of d is shown in Fig. 4(b). The solid line is the exact calculation and the dotted line is based on Eq. (14). The agreement is fairly good, and only oscillation with a long period was observed. For the analytical model calculation, we included only the extremal spanning vector at $k_\parallel = 0$ and ignored the contribution from the extremal point at $k_\parallel = 0.68 k_F$. This is because the tunneling probability decreases rapidly away from $k_\parallel = 0$ and the spin asymmetry of the transmission coefficient ($|t_\uparrow^L|^2 - |t_\downarrow^L|^2$) is very small at $k_\parallel = 0.68 k_F$. The observed behavior clearly shows that even though there are two possible periods of the TMR oscillation from the Fermi surface of the NM, only the period with significant spin asymmetry of the
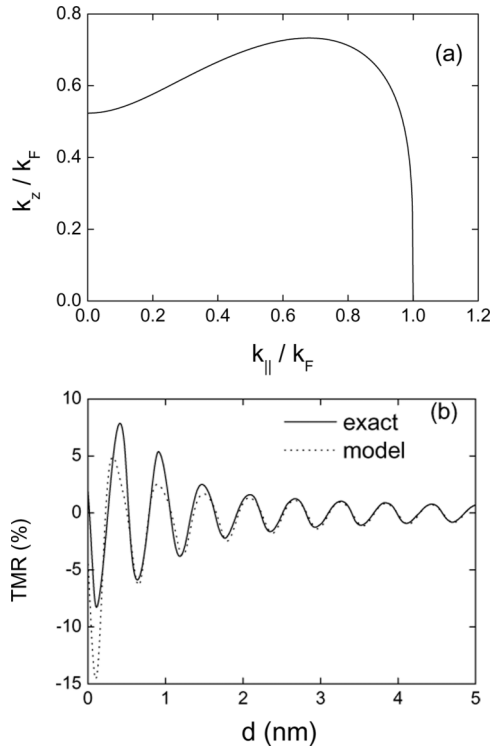
FIG. 4. (a) Cross section of the Fermi surface for the NM spacer with the dispersion relation given in Eq. (15). $k_F = \sqrt{2m_0\varepsilon_F}/\hbar$ is the Fermi wave vector for the majority spin of the FM layer. It is similar to the Cu(001) case. (b) TMR as a function of the NM layer thickness d. Except for the NM spacer, the other parameters are the same as those used in the previous case. The solid line is the exact result, and the dotted line is based on the proposed analytical formula.

transmission coefficient would survive. The case of multiple extremal spanning vectors in the NM layer is also described well by our analytical formula.

C. Tunnel barrier with nonparabolic dispersion relation

Third, we studied the case that the point for the maximum tunneling probability does not coincide with the position of the extremal spanning vector of the NM Fermi surface in $\mathbf{k}_\parallel$ space. We assumed that the dispersion relation of the tunnel barrier is given by

$$\varepsilon = \left[\frac{\hbar^4 \left(k_x^2 - a^2 k_F^2\right)^2}{4m_0^2} + \frac{\hbar^4 \left(k_y^2 - a^2 k_F^2\right)^2}{4m_0^2} + V_\parallel^2 \right]^{1/2}$$
$$+ \frac{\hbar^2 k_z^2}{2m_0} + V_B - V_\parallel, \qquad (16)$$

where V_B is the bottom energy of the tunnel barrier, $V_\parallel$ is an energy parameter, and k_F is the magnitude of the Fermi wave vector for the NM material. With this tunnel barrier, the tunneling probability is highest at $\mathbf{k}_\parallel = (ak_F, ak_F)$. For the calculation, we used $b = 1.5$ nm, $V_B = 6$ eV, $V_\parallel = 0.7$ eV, and $a = 0.566$. The other materials are assumed to be the same as in Sec. III A. The dispersion relation of the FM material is given by $\varepsilon(\mathbf{k}) = \hbar^2 k^2/2m_\sigma^* + V_\sigma$ with $V_\uparrow = 0$, $V_\downarrow = \Delta$, $m_\uparrow = m_0$, and $m_\downarrow^* = m_0 \varepsilon_F/(\varepsilon_F - \Delta)$. The dispersion relation of the NM material is the same as that of the FM material for
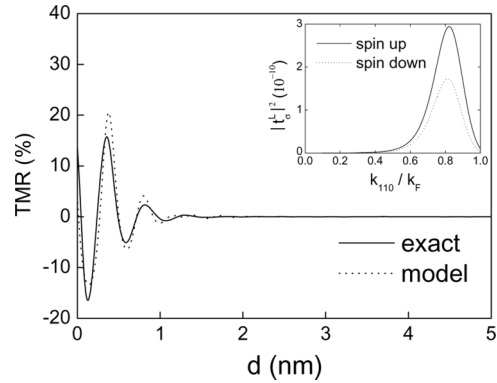

FIG. 5. TMR as a function of the NM layer thickness d when the point for the maximum transmission coefficient of the tunnel barrier does not coincide with the extremal point of the NM Fermi surface in $\mathbf{k}_\parallel$ space. The dispersion relation of the tunnel barrier is given in Eq. (16), and the FM and NM materials are assumed to be the same as in Fig. 3. The inset is the transmission coefficient as a function of $\mathbf{k}_\parallel$ along the [110] orientation for the FM/I/NM system.

majority spin. Note that the extremal spanning vector of the NM Fermi surface is located at $\mathbf{k}_\parallel = 0$. The parameters used in the calculation are $\varepsilon_F = 4$ eV and $\Delta = 2.5$ eV. The TMR dependence on the thickness of the NM layer is displayed in Fig. 5. The solid line is the exact result and the dotted is the result of our analytical formula. As expected, the TMR decays faster and it is almost negligible when the NM layer is thicker than about 2 nm. The inset is the transmission coefficient as a function of $\mathbf{k}_\parallel$ along the [110] direction for the FM/I/NM system. It has the maximum value around $k_{110} = 0.8 k_F$, at which we have $\nabla_{\mathbf{k}_\parallel}(\chi) = 0$. On the other hand, the spanning vector (q) of the NM Fermi surface has the longest at $\mathbf{k}_\parallel = 0$. The maximum point of the tunneling probability does not coincide with the extremum of the NM Fermi surface, and the extremal point is determined from $\nabla_{\mathbf{k}_\parallel}[-b\chi + i(qd + \phi)] = 0$. The extremal point is d dependent and a complex number. It is not easy to calculate the d-dependent extremal point exactly and we used the following approximation. At the Fermi level, k_z in Eq. (16) is an imaginary number ($k_z = i\kappa$). We used a parabolic function of κ which was expanded in a Taylor series around $\mathbf{k}_\parallel = (ak_F, ak_F)$. The calculation became much simpler, and the extremal point and the corresponding vector q_α in Eq. (13) were obtained immediately as functions of d. In the range of thin NM layers with significant TMR, q_α is shorter than $2k_F$, the extremal spanning vector of the NM Fermi surface. Thus, the oscillation period in this region is longer than what is expected from the NM Fermi surface. Whenever the extremal spanning vectors of the NM Fermi surface are significantly away from the point of the maximum transmission coefficient in the $\mathbf{k}_\parallel$ space, we expect rapid decay of TMR as a function of the NM thickness.

D. Free-electron model

Finally, we investigated the free-electron model case, where all the effective masses are simply the bare electron mass m_0. The NM band is assumed to be the same as the majority-spin band of FM, which is commonly adopted in the theoretical calculations. The parameters used in the calculation are
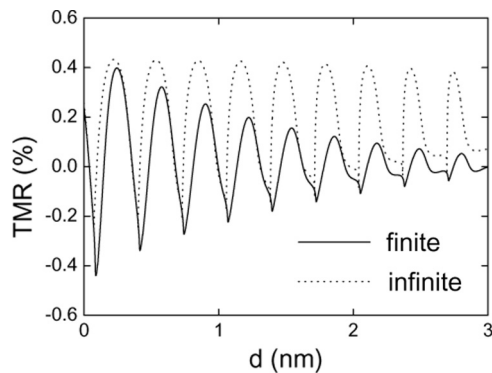
FIG. 6. TMR as a function of the NM layer thickness d for the free-electron band. The parameters used in the calculation are $\varepsilon_F = 4$ eV, $V_I = 6$ eV, $\Delta = 3.5$ eV, and $b = 1$ nm. The solid line is for the 1-nm FM layer and the dotted line is for the infinite FM layer.

$\varepsilon_F = 4$ eV, $V_I = 6$ eV, $\Delta = 3.5$ eV, and $b = 1$ nm. A plot of the TMR dependence on NM thickness is displayed by a dotted line in Fig. 6. In this case, the TMR reaches a finite value when the NM thickness becomes infinite. At first sight, this seems to contradict our analytical formula Eq. (14) given in Sec. II. The reason for finite TMR at infinite d can be explained as follows. We obtained $k_z = \sqrt{2m_0(\varepsilon_F - \Delta)/\hbar^2 - k_\parallel^2}$ from the dispersion relation at the Fermi level. When the magnetizations of the FM layers are antiparallel, electrons with the majority spin in the FM(L) layer do not penetrate to the FM(R) layer for $k_\parallel > \sqrt{2m_0(\varepsilon_F - \Delta)}/\hbar$ because k_z becomes imaginary in the FM(R) layer. The electrons with the majority spin for $k_\parallel > \sqrt{2m_0(\varepsilon_F - \Delta)}/\hbar$ in the FM(L) layer are totally reflected at the NM/FM(R) interface due to the potential step and do not contribute to conduction. Thus, G_{AP} is underestimated and gives rise to a finite ΔG and consequently a finite TMR, even when the NM layer is infinite, as long as the transport is coherent. This is more pronounced for a larger Δ, lower barrier height, and thinner tunneling barrier because a larger portion of electrons with the Fermi energy will be completely reflected at the NM/FM(R) interface. When deriving Eq. (13) in Sec. II, we considered multiple reflection inside the NM layer to calculate the transmission, and we assumed that once the electrons tunnel through the tunnel barrier, most of them flow to the FM(R) layer after multiple reflections. However, in the AP magnetizations of FM layers of the free-electron model, the electrons with majority spin for $k_\parallel > \sqrt{2m_0(\varepsilon_F - \Delta)}/\hbar$ in the FM(L) layer cannot penetrate into the FM(R) layer after tunneling because of the potential step, resulting in a finite TMR for the infinite NM layer. To clarify this point, we calculated the TMR for the finite FM(R) layer; namely, the FM(L)/I/NM/FM(R)/NM junctions. The FM(R) layer is 1 nm thick, and the result is shown by the solid line in Fig. 6. The FM(R) layer behaves like a potential barrier for electrons with the majority spin and $k_\parallel > \sqrt{2m_0(\varepsilon_F - \Delta)}/\hbar$ in the FM(L) layer. However, the TMR goes to zero as the NM thickness increases. When the FM(R) layer is not too thick, the tunneling probability through this potential barrier is larger than that through the tunnel barrier (I), and most of electrons with majority spin and $k_\parallel > \sqrt{2m_0(\varepsilon_F - \Delta)}/\hbar$ in the FM(L) layer eventually flow to the NM(R) layer once they tunnel

through the insulating barrier. Even for the infinite FM(R) layer, the TMR for the infinite NM layer becomes negligible as Δ increases, the thickness of the tunnel barrier increases, and the barrier height increases. This is because only a small portion of electrons with the Fermi energy will be completely reflected at the NM/FM(R) interface. Also, if the minority spin band of the FM layer is set to be the same as the NM band, the TMR goes to zero as the NM thickness increases because there is no total reflection at the NM/FM(R) interface. The finite TMR for the infinite NM layer is possible when a significant portion of electrons with the Fermi energy have less transmission probability into the FM(R) layer than that through the tunnel barrier. Complete reflection of electrons at the interface between two metals may occur for some given $\mathbf{k}_\parallel$ at the Fermi level due to the mismatch of the electronic states. However, even slight scattering would lead to the penetration of electrons into the FM(R) layer. In this sense, we do not expect that a large portion of electrons with Fermi energy are reflected completely, in reality, at the NM/FM interface. Thus, it is unrealistic to expect a finite TMR as the NM thickness increases in experiments.

IV. CONCLUSION

We calculated the TMR of FM/I/NM/FM tunnel junctions. The TMR was calculated as a function of NM thickness using the Landaur-Büttiker formula. Multiple band structures were included and an analytical form describing the TMR was obtained. Conductance was calculated from the summation of the transmission over $\mathbf{k}_\parallel$. The transmission was obtained by considering multiple reflections between the I/NM and NM/FM interfaces. The summation over $\mathbf{k}_\parallel$ was carried out analytically. The contribution was mainly from the extremal point in $\mathbf{k}_\parallel$ space that was determined from the combination of the NM Fermi surface and the $\mathbf{k}_\parallel$ dependence of the transmission coefficient of the FM/I/NM junction. The TMR was expressed with the transmission coefficient of the FM/I/NM junction, reflection amplitudes at the NM/I and NM/FM interfaces at the Fermi level, and the extremal wave vector. Many oscillation periods can be inferred from the shape of the NM Fermi surface, but they can be observed only when the corresponding spin asymmetry of the transmission coefficient is significant. We suggest that only few oscillation periods are likely to be observed in real experiments. When the NM spacer is thin, our proposed model indicates that the decay of the TMR was slower than the inverse of the space thickness for coherent transport.

Numerical calculations were performed to investigate the accuracy of the proposed formula. An envelope-function theory was adopted, and our model was compared to the exact result. We showed that the results of the proposed formula are in good agreement with the exact calculations. The TMR dependence on the thickness of the NM spacer was affected by the tunnel barrier thickness, which was well described by our formula. The numerical calculation was extended to the case with multiple extremal spanning vectors in the Fermi surface of the NM spacer. Our proposed formula is in good agreement with the exact result, and only the oscillation period with significant spin asymmetry of the transmission coefficient was observed as predicted using our formula. When the tunneling

probability associated with each extremal spanning vectors of the NM Fermi surface is low, the TMR decays very fast as the NM thickness increases. A free-electron case was also considered. The NM band was assumed to be the same as the majority spin band of the FM layer, and spin splitting in the FM layer was assumed to be rather large. The TMR approached a finite value as the NM thickness increased. This was because a large portion of electrons with the majority spin in the left FM layer were reflected completely at the right NM/FM interface. When the semi-infinite FM layer on the right side was replaced by a finite layer, the TMR decayed to zero as the NM thickness increased. As long as the transmission into the FM layer was higher than that through the tunnel barrier, the TMR became zero as the thickness of the NM spacer increased. We suggest that finite TMR for the infinite NM spacer is unrealistic in real experiments.

*chan@inha.ac.kr

[1] J. S. Moodera, L. R. Kinder, T. M. Wong, and R. Meservey, Phys. Rev. Lett. **74**, 3273 (1995).

[2] S. Yuasa and D. D. Djayaprawira, J. Phys. D **40**, R337 (2007).

[3] A. Vedyayev, N. Ryzhanova, C. Lacroix, L. Giacomoni, and B. Dieny, Europhys. Lett. **39**, 219 (1997).

[4] P. LeClair, H. J. M. Swagten, J. T. Kohlhepp, R. J. M. van de Veerdonk, and W. J. M. de Jonge, Phys. Rev. Lett. **84**, 2933 (2000).

[5] P. LeClair, J. T. Kohlhepp, H. J. M. Swagten, and W. J. M. de Jonge, Phys. Rev. Lett. **86**, 1066 (2001).

[6] S. Zhang and P. M. Levy, Phys. Rev. Lett. **81**, 5660 (1998).

[7] S. Yuasa, T. Nagahama, and Y. Suzuki, Science **297**, 234 (2002).

[8] H. Itoh, J. Inoue, A. Umerski, and J. Mathon, Phys. Rev. B **68**, 174421 (2003).

[9] H. Itoh, J. Inoue, A. Umerski, and J. Mathon, J. Magn. Magn. Mater. **272-276**, e1467 (2004).

[10] A. A. Shokri and A. Saffarzadeh, J. Phys.: Condens. Matter **16**, 4455 (2004).

[11] Z. M. Zeng, X. F. Han, W. S. Zhan, Y. Wang, Z. Zhang, and S. Zhang, Phys. Rev. B **72**, 054419 (2005).

[12] J. Yang, J. Wang, Z. M. Zheng, D. Y. Xing, and C. R. Chang, Phys. Rev. B **71**, 214434 (2005).

[13] Z. P. Niu, Z. B. Feng, J. Yang, and D. Y. Xing, Phys. Rev. B **73**, 014432 (2006).

[14] X. Feng, O. Bengone, M. Alouani, I. Rungger, and S. Sanvito, Phys. Rev. B **79**, 214432 (2009).

[15] S.-P. Chen and C. R. Chang, IEEE Trans. Magn. **45**, 2410 (2009).

[16] G. Autes, J. Mathon, and A. Umerski, Phys. Rev. B **80**, 024415 (2009).

[17] S.-P. Chen, J. Appl. Phys. **107**, 09C716 (2010).

[18] S.-P. Chen, Thin Solid Films **519**, 8215 (2011).

[19] B. C. Lee, J. Appl. Phys. **107**, 09C708 (2010).

[20] H. Bruus and K. Flensberg, *Many-Body Quantum Theory in Condensed Matter Physics* (Oxford University Press, New York, 2004).

[21] B. Lee and Y.-C. Chang, Phys. Rev. B **52**, 3499 (1995).

[22] B. C. Lee and Y.-C. Chang, Phys. Rev. B **62**, 3888 (2000).

[23] M. D. Stiles, J. Magn. Magn. Mater. **200**, 322 (1999), and references therein.

[24] L. Tsetseris, B. C. Lee, and Y.-C. Chang, Phys. Rev. B **55**, 11586 (1997).

[25] C.-Y. You, C. H. Sowers, A. Inomata, J. S. Jiang, S. D. Bader, and D. D. Koelling, J. Appl. Phys. **85**, 5889 (1999).

[26] T. Nagahama, S. Yuasa, E. Tamura, and Y. Suzuki, Phys. Rev. Lett. **95**, 086602 (2005).

[27] R. Matsumoto, A. Fukushima, K. Yakushiji, S. Nishioka, T. Nagahama, T. Katayama, Y. Suzuki, K. Ando, and S. Yuasa, Phys. Rev. B **79**, 174436 (2009).